

Discovery of Potent and Selective Histone Deacetylase Inhibitors via Focused Combinatorial Libraries of Cyclic $\alpha_3\beta$ -Tetrapeptides

Christian A. Olsen and M. Reza Ghadiri*

Department of Chemistry and The Skaggs Institute for Chemical Biology, The Scripps Research Institute, 10550 North Torrey Pines Road, La Jolla, California 92037

Received June 10, 2009

Histone deacetylase (HDAC) inhibitors are powerful tools in understanding epigenetic regulation and have proven especially promising for the treatment of various cancers, but the discovery of potent, isoform-selective HDAC inhibitors has been a major challenge. We recently developed a cyclic $\alpha_3\beta$ -tetrapeptide scaffold for the preparation of HDAC inhibitors with novel selectivity profiles (*J. Am. Chem. Soc.* 2009, 131, 3033). In this study, we elaborate this scaffold with respect to side chain diversity by synthesizing *one-bead–one-compound* combinatorial libraries of cyclic tetrapeptide analogues and applying two generations of these focused libraries to the discovery of potent HDAC ligands using a convenient screening platform. Our studies led to the first HDAC6-selective cyclic tetrapeptide analogue, which extends the use of cyclic tetrapeptides to the class II HDAC isoforms. These findings highlight the persistent potential of cyclic tetrapeptides as epigenetic modulators and possible anticancer drug lead compounds.

Introduction

Histone deacetylases (HDACs^e) are a family of enzymes found in bacteria, fungi, plants, and animals that profoundly affect cellular function. The natural substrates of most HDACs are believed to be N^e-acetyl lysine residues in the tails of histones H2A, H2B, H3, and H4 (Supporting Information (SI) Figure S1). The degree of acetylation of these sites affects the packing of nucleosomes in chromatin complexes as well as the recruitment of transcription activator- and repressor-proteins to histone tails, which in turn modulate the extent of gene transcription.^{1–4} The HDAC enzymes are not restricted to deacetylation of histones, however, and are known to regulate the function of other proteins within cells.⁵ For example, HDAC6 has been associated with deacetylation of α -tubulin⁶ as well as peroxiredoxin I and II⁷ and has been shown to rescue neurodegeneration in *Drosophila melanogaster*.⁸ To date, 11 Zn²⁺-dependent human HDAC enzymes have been identified and classified according to their sequence similarity (class I: HDACs 1, 2, 3, and 8; class IIa: HDACs 4,

5, 7, and 9; class IIb: HDACs 6 and 10; class IV: HDAC11). Class III HDACs comprise a series of NAD⁺-dependent enzymes (sirtuins 1–7).

Although the majority of HDAC inhibitors in clinical trials are nonselective,^{9,10} small-molecule HDAC inhibitors have proven to be promising candidates for therapeutic intervention, especially as tumor suppressors for potential cancer chemotherapies.^{3,11–15} Indeed, several candidates have advanced to clinical trials⁹ and vorinostat/SAHA was recently approved by the FDA for the treatment of cutaneous T-cell lymphoma.¹⁶ Nonselective HDAC inhibitors have also recently been shown to elicit positive effects related to neurological disorders.^{17–20} Despite these successes with nonselective HDAC inhibitors, the ability to *selectively* perturb individual HDACs with small molecules would be exceedingly useful in unravelling the complex and highly dynamic network of HDAC signaling and in the design of new and safer drug candidates. Structure-based efforts to design class- or isoform-selective inhibitors have been hampered by the limited structural information available. To date, there is only a structural understanding of "HDAC-Like Protein" (HDLP),²¹ HDAC8,^{22,23} and the catalytic domains of HDAC7²⁴ and HDAC4.²⁵ Although the class IIa HDACs have considerably lower intrinsic deacetylase activity compared to class I HDACs against standard substrates,^{4,26–28} class IIa HDACs play pivotal roles in numerous pathways and they are therefore equally important targets for future selective therapeutic intervention in various diseases.^{4,29–32}

Nature provides a number of related cyclic scaffolds with HDAC inhibitory activity, including nonribosomal depsipeptides,³³ the marine natural product largazole,^{34–39} and tetrapeptide natural products such as the trapoxins,^{40,41} HC toxins,^{42,43} chlamydocin,⁴³ apicidins (**1**),^{44–46} and the azumamides (**2**)^{47–51} (Figure 1). Numerous analogues of these

*To whom correspondence should be addressed. Phone: (+1) 858-784-2700. Fax: (+1) 858-784-2798. E-mail: ghadiri@scripps.edu.

^a Abbreviations: AMC, 7-amino-4-methylcoumarin; Aoda, (S)-2-amino-8-oxo-decanoic acid; Asu, (S)-2-amino-suberic acid; DIC, N,N'-diisopropylcarbodiimide; FBS, fetal bovine serum; Fmoc, fluorenylmethyloxycarbonyl; HATU, 2-(1H-azabenzotriazol-1-yl)-1,1,3,3-tetramethyluronium hexafluorophosphate; HDAC, histone deacetylase; HDLP, HDAC-like protein; HOBt, hydroxybenzotriazole; HPLC, high performance liquid chromatography; MALDI-TOF, matrix-assisted laser desorption/ionization time-of-flight; MS, mass spectrometry; NAD, nicotinamide adenine dinucleotide; Nal, 1-naphthylalanine; NCoR2, nuclear coreceptor 2; NMR, nuclear magnetic resonance; Pa, 3-propanoic acid; Pip, pipercolic acid; PMS, N-methyl-di-benzopyrazine methyl sulfate; SAR, structure–activity relationship; SPPS, solid-phase peptide synthesis; SPS, solid-phase synthesis; TFA, trifluoroacetic acid; TSA, trichostatin A; XTT, 3'-[1-(phenylamino-carbonyl)-3,4-tetrazolium]-bis-(4-methoxy-6-nitro)-sulfonic acid.

natural compounds have been investigated as well.^{52–63} For the medicinal chemist, cyclic tetrapeptides built from all α -amino acids often present significant challenges as drug targets due to poor macrolactamization yields for closing the 12-membered ring and multiple three-dimensional conformations on the NMR time scale.^{64–66} We were recently able to minimize these shortcomings by developing synthetic HDAC inhibitor scaffolds (**3**, Figure 1) that have an α - β -amino acid substitution in the backbone to give a 13-membered ring.⁶⁷ By systematically changing the chirality of the amino acids and the position of the β -amino acid, we optimized the scaffold for inhibition of HeLa extract HDAC activity. Moreover, we correlated compound potencies with their high-resolution NMR structures, which allowed us to construct a three-dimensional pharmacophore model. In our previous study, the identities of the side chains were fixed so that we could focus on understanding the effects of peptide backbone modifications on structure and potency. In contrast, here we investigate a variety of side chain functionalities by designing and carrying out total solid-phase synthesis (SPS) of *one-bead-one-compound* libraries⁶⁸ of cyclic peptides for the purpose of inhibiting HDAC enzymes. The present study focuses on HDACs with potent deacetylase activity against histones and standard substrates, i.e., class I HDACs 1, 3, and 8 as well as class IIb HDAC6. HDAC2 was omitted from this investigation due to its high degree of sequence similarity to HDAC1.

Results and Discussion

Preliminary SAR Information. To guide the design of the first-generation library, we initially surveyed the effect of the Zn^{2+} -coordinating group and its distance from the peptide core on our selection of HDAC enzymes. Although we had previously established that changing the Zn^{2+} -coordinating functionality in peptides **3a–c** accommodated leaps in potency using HeLa cell nuclear extract,⁶⁷ we wished to determine more specifically how the inhibitors acted against the individual HDAC isoforms. We therefore tested **3a–c** against our panel of recombinant human HDACs as well as against a HeLa cell cytosolic extract (Table 1). The inhibition trend described previously for **3a–c** against HeLa nuclear extract (hydroxamic acid > ethylketone > acid Zn^{2+} -coordinating functionality) was also observed for the cytosolic extract as well as for HDACs 1 and 3. The IC_{50} values indicated that the predominant source of HDAC activity in HeLa nuclear extract is HDAC1, while HDAC3 seems to be more dominant in HeLa cytosolic extract, which corresponds well with the fact that HDAC3 is known to shuttle into the cytoplasm.⁶⁹ Furthermore, the observed IC_{50} values indicated that the requirements for inhibition of HDAC8 are different from the other HDACs in class I, in agreement with previous findings.^{10,22,23} Interestingly, ketone **3b**, like apicidin, did not inhibit HDAC6 in the concentration range tested, while acid **3a** proved to be a micromolar inhibitor of HDAC6. This might be explained by an interaction between the carboxylate of **3a** and a free binding site His in HDAC6 (SI Figure S2). For comparison, HDAC8 contains an active site His residue (His143) that forms a contact with an adjacent Asp (Asp183). Although HDAC6 does contain a corresponding active site His residue, the corresponding Asp is absent, so it is possible that the active site His in HDAC6 is free to interact with the carboxylate in **3a** (SI Figure S2). This

finding was encouraging because the carboxylic acid Zn^{2+} -coordinating group would provide a useful handle for resin anchoring to synthesize focused libraries of inhibitors via efficient and robust chemical SPS techniques.

To reduce the synthetic effort required for assessing the effect of different lengths of the Zn^{2+} -coordinating side chain, we designed a series of alkylated cysteine-derived analogues (**4a–d**), which enabled evaluation of the distance requirements for the different enzyme isoforms (Figure 1 and SI Figure S3). The use of alkylated cysteine containing compounds has precedence in the literature for probing HDACs.^{70,71} It was previously shown that changing the linker length by plus/minus one methylene unit significantly decreased the potency of inhibition of HDAC activity in HeLa cell extract;⁵² however, the effect on individual HDAC isoforms was not investigated in that study. Furthermore, largazole analogues with different linker lengths have recently been investigated.⁶¹ With the sulfur atom in compound **4a** extending the linker length by only ~ 0.28 Å compared to the methylene in **3b**, it was not surprising to find that this compound behaved similarly to **3b**. The corresponding compound with a linker of one fewer methylene unit, **4b**, showed total loss of activity. Likewise, the shortened linkers in the carboxylic acids **4c** and **4d** also rendered these peptides less potent than their parent compound (**3a**) across our selection of enzymes. It may be noted, however, that a comparison of compounds **3a** vs **4c** reveals a ~ 40 -fold decrease in potency against HDAC1 and only a ~ 3 -fold decrease against HDAC8. The length of the linker may thus be a factor to consider when designing isoform selective HDAC ligands. The design of so-called “linkerless” hydroxamic acid HDAC inhibitors with selectivity for HDAC8 was recently reported,⁷² supporting the suggestion that shortened linkers might prove effective against this isoform. Partial decomposition of these thioether compounds was observed upon prolonged storage (presumably due to oxidation of the thioether); nonetheless, they are useful as a discovery tool giving easy access to a variety of different linker lengths and Zn^{2+} -coordinating moieties.

First-Generation Library Design. Our first-generation library comprised a focused 252-member *one-bead-one-compound* library aimed at exploring the importance of the side chain functionalities for potent HDAC inhibition. On the basis of our preliminary studies and to facilitate solid phase synthesis, we opted to employ the carboxylic acid Zn^{2+} -coordinating residue for this library. Albeit not the most potent Zn^{2+} -coordinating moiety, the carboxylic acid was considered more appropriate than the hydroxamic acid because the latter gave rise to poor isoform selectivity for the cyclic tetrapeptides tested.⁵² The ethylketone containing ligands seemed ideal for inhibition of class I HDACs 1–3 but showed no inhibitory activity against HDAC6, and the total solid-phase synthetic route to give the ethylketone containing ligands required postcleavage purification (SI Figure S4), which was not ideal for a high-throughput library screening scheme.

Previous SAR studies involving cyclic tetrapeptides as HDAC inhibitors have indicated that the aromatic residue vicinal to the Zn^{2+} -coordinating amino acid (position aa2 in Figure 2) is important for potent inhibition.^{58,59} We therefore decided to probe this position extensively in our initial library. Aromatic residues of varied bulkiness and polarity as well as nonaromatic hydrophobic residues were included. For position aa3, four different β^3 -amino acids were chosen,

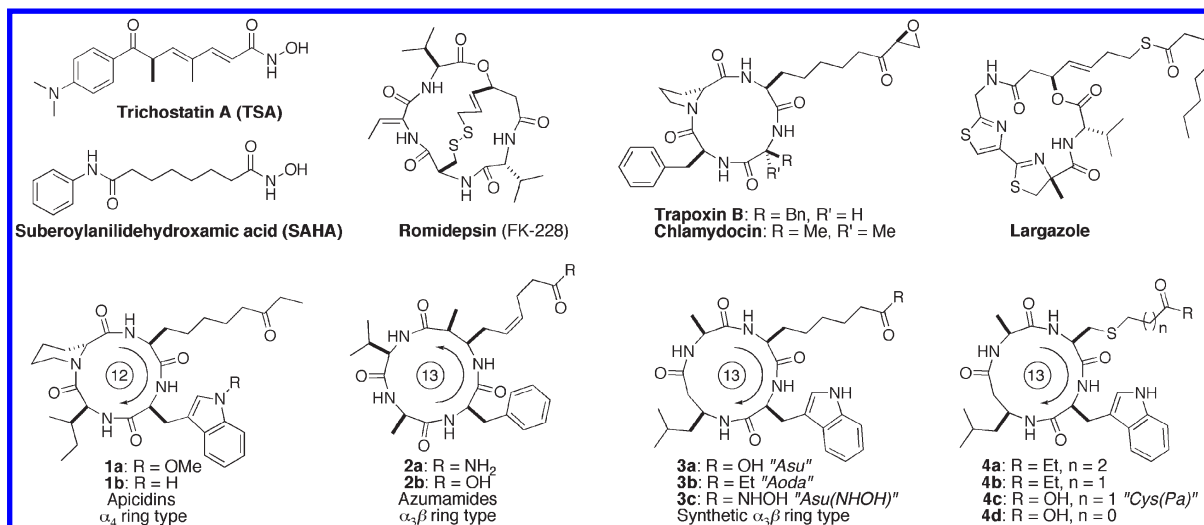


Figure 1. HDAC inhibitors, natural products, and scaffolds. Arrows show the amide chain directionality. Scaffold 3 shows the structure of our previously developed $\alpha_3\beta$ ring type. Compound 4 is based on the optimized synthetic $\alpha_3\beta$ ring type but contains a cysteine residue that readily allows for introduction of different Zn^{2+} -coordinating moieties.

Table 1. Potencies of 3a–3c, 4a–d, Apicidin, and TSA against HeLa Extracts and Recombinant Enzymes (IC_{50} [nM])^a

compd	HeLa extracts		class I			class IIb
	nuclear	cytosolic	HDAC1	HDAC3 ^b	HDAC8	HDAC6
3a	324 ± 4	630 ± 30	116 ± 4	608 ± 3	2300 ^c	2310 ± 20
3b	19 ^c	85 ± 6	26 ± 3	143 ± 10	2200 ^c	> 10000
3c	< 1 ^c	3 ± 1.5	2 ± 1.4	18 ± 3	133 ^c	31 ± 2
4a	54 ^c	54 ± 5	(20)	62 ± 7	(4920)	> 10000
4b	ND ^c	ND	> 10000	> 10000	> 10000	> 10000
4c	ND	ND	(4840)	(7080)	(6050)	> 10000
4d	ND	ND	> 10000	> 10000	(9700)	> 10000
1a apicidin	22 ± 6	43 ± 8	22 ± 4	29 ± 4	760 ± 20	> 10000
TSA ^d	3 ± 1.3	3 ± 1.0	3.3 ± 1.5	11 ± 1.4	25 ± 3	6 ± 1.9

^a IC_{50} values are means of at least two experiments performed in duplicate unless otherwise noted. Values in parentheses are from a single assay performed in duplicate. ^bIn complex with NCoR2. ^cFrom our previous report.⁶⁷ ^dTSA (trichostatin A) was included as a positive control inhibitor in the assays with HDAC6 and HDAC8 because apicidin is not a potent inhibitor of these enzymes. ^eND = not determined.

including a β^3 -Phe residue to mimic the Phe side chain found in trapoxin and chlamydocin. Residues commonly found in natural product HDAC inhibitors (e.g., Aib, D-Pip, Pro, and Val) were included along with Phe at position aa4. To synthesize the library, the first residue (*N*-Fmoc-(*S*)-Asu-O-Allyl) was anchored to a macrobead 2-chlorotrityl solid support via its carboxylic acid side chain using protocols previously developed for regular SPS resins.^{67,73} The choice of macrobeads as solid support afforded facile handling during the split–pool synthesis procedure and enabled an economical small-scale preparation of each compound while still affording enough material to test each product in several assays in 96-well microtiter plates (Figure 2). After the total synthesis of the 252-member library of ligands including on-resin cyclization, individual beads were arrayed in 96-well plates, cleaved by treatment with a cocktail containing trifluoroacetic acid (TFA), and dissolved in DMSO to give stock solutions. After screening the library for HDAC inhibitory activity using HeLa nuclear extract, the obtained hits were analyzed and sequenced using an LC-MS/MS procedure previously developed in our lab.⁷⁴

From the initial screen and retesting of the first-generation library for inhibition of HDAC activity in HeLa cell extract,

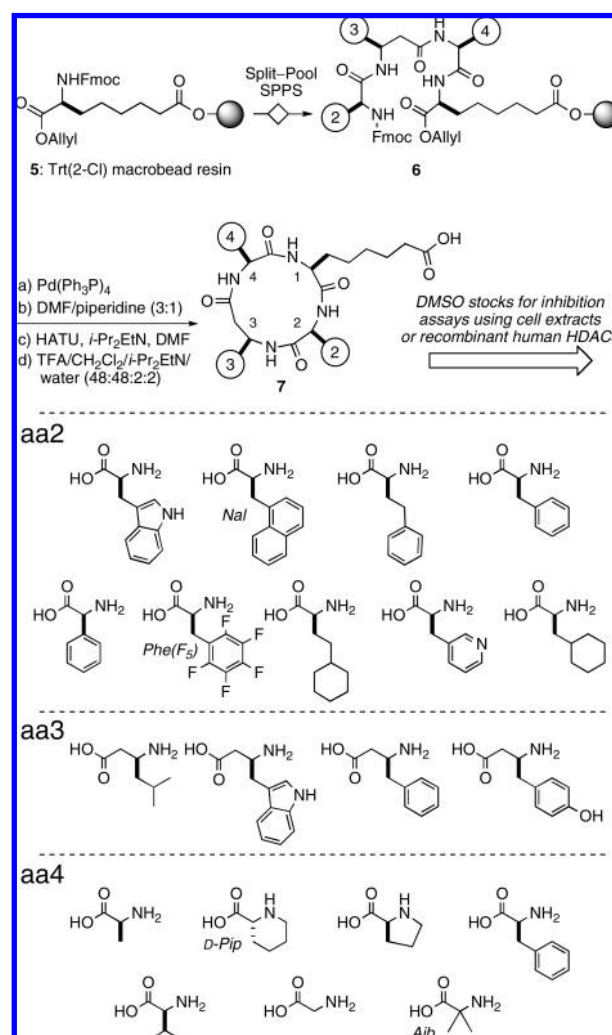


Figure 2. Synthetic scheme and amino acids used in the first-generation library.

we obtained eight confirmed hits (six different structures) as shown in Figure 3A. Semilogarithmic plots were obtained from the inhibition data at two different dilutions of the

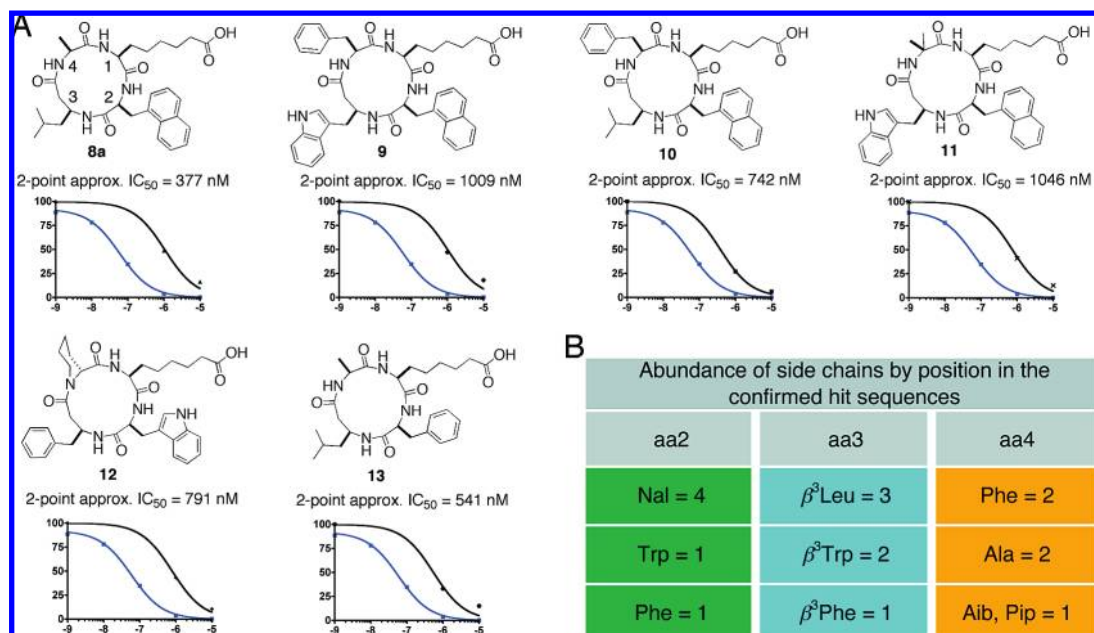


Figure 3. First-generation library screening results. The library screening in 96-well plates initially provided 15 “hits” that satisfied a criteria of $>75\%$ inhibition at $10\ \mu\text{M}$ and $>25\%$ inhibition at $1\ \mu\text{M}$ against HeLa cell extract. Identified hits were then retested in duplicate and sequenced using LC–MS/MS, which confirmed six different hit structures. (A) Structures of hits and approximate IC_{50} values were obtained from plots of the inhibition data; the dose–response curve for apicidin (blue) is shown in each plot for comparison. (B) Table showing the abundance of amino acids by position in the hit series.

initial stock solutions, from which approximate IC_{50} values for these peptides were calculated using GraphPad Prism. Interestingly, the two most potent compounds (**8a** and **13**) closely resembled our parent compound (**3a**), having only a single substitution in the aromatic residue at the aa2 site (Trp→naphthylalanine in **8a** or Trp→Phe in **13**). Furthermore, one of the hits with intermediate potency (compound **12**) contained both the aa2–Trp and the aa4–D–Pip residues as found in the natural product apicidin A (**1b**). The abundance of the various side chains by position on the scaffold (Figure 3B) revealed that the aa2 position required an aromatic side chain as anticipated; the naphthylalanine residue, which is similar to Trp in size, was the most abundant in the hit series. At position aa3, the β^3 Leu residue was more abundant than the aromatic residues included in the library, and at position aa4, no consensus could be derived, indicating that the identity of the side chain at this position is less significant for inhibition of HeLa cell HDAC activity.

To confirm the results from the library screening, the four identified naphthylalanine containing compounds (**8a**, **9–11**) were resynthesized on $\sim 50\ \mu\text{mol}$ scale, purified, and retested to obtain IC_{50} values against HeLa nuclear extract (Table 2). Their IC_{50} values confirmed the approximated values from the initial screening data, supporting that the library screening format is appropriate for the discovery of novel HDAC inhibitors. To derive more detailed SAR information from this initial hit series, compound **14** was also prepared along with the ethylketone analogue (**8b**) of compound **8a** (SI Figure S5 and Table 2). The unnatural naphthylalanine residue was confirmed to be a good alternative to Trp at position aa2. Furthermore, the relative IC_{50} values for carboxylic acid (**8a**) vs ethylketone (**8b**) showed the expected trend, as ethylketone **8b** was 10–30-fold more potent against HeLa extract and HDACs 1 and 3. A decrease in potency was observed for HDAC6, providing further evidence that ketones are not favorable for inhibition of this

enzyme isoform. The SAR also suggested that aromatic side chains at position aa3 are not favorable for inhibition of class I HDACs (**9** vs **10** and **11** vs **14**). Interestingly, compound **10** was 2-fold more potent against HDAC1 compared to our parent carboxylic acid (**3a**) and was somewhat less potent against HDAC3, thus providing a ~ 10 -fold selectivity index for HDAC1 vs HDAC3 as well as potent inhibition of HDAC1 (68 nM). The substitution of the Ala→Phe residue in position aa4 may therefore give rise to an increased selectivity for HDAC1.

Compounds **15** and **16**, in which the least structurally restrictive residue (aa4) was substituted with *N*^ε-Ac-lysine or Aoda, respectively, were also prepared and tested (Table 2) so that we could ascertain how such substitutions would influence binding to the HDACs before designing a second-generation library. The aa4-Lys(Ac) residue in compound **15** was inspired by the two consecutive lysine residues K381 and K382 known to be involved in acetylation/deacetylation events in the transcription factor p53. Moreover, the Lys(Ac)-Lys(Ac) motif has been used in a commercially available fluorescent HDAC8 substrate (His-Arg-Lys(Ac)-Lys(Ac)-AMC, www.biomol.com), which led us to hypothesize that such a motif might provide an improved degree of recognition by HDAC8. The Aoda–Aoda sequence in **16** provides a double isosteric version of this feature. Indeed, improved activity against HDAC8 was observed for compound **15** (150 nM) and to a much lesser extent for **16** (1400 nM); however, the IC_{50} values for inhibition of HDACs 1 and 3 were still in the same range as that observed for parent compounds **3b** and apicidin (Table 2).

Second-Generation Library Design, Synthesis, and Screening. On the basis of the SAR information gathered from the first-generation library, we decided to focus on the diversification of the aa3 and aa4 positions in the second-generation library in the hopes of reducing bias for class I HDAC inhibitory activity. In addition to amino acids found in the

Table 2. IC₅₀ Values [nM] of Purified Compounds against HeLa Nuclear Extract and Recombinant Enzymes^a

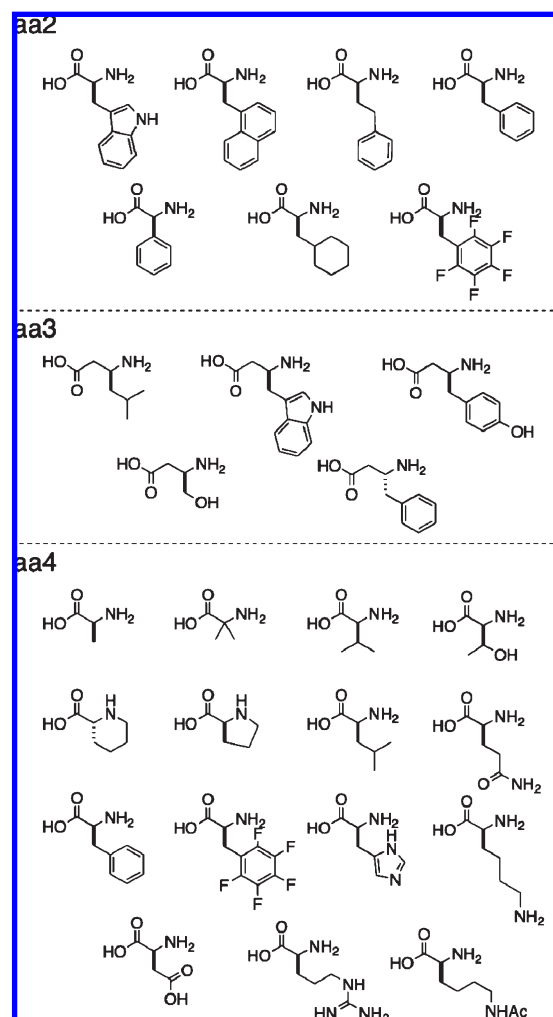
compd	HeLa nuclear extract	class I			class IIb
		HDAC1	HDAC3 ^b	HDAC8	HDAC6
8a c[Asu-Nal-β ³ Leu-Ala]	205 ± 5	200 ± 10	990 ± 20	ND	4900 ± 70
8b c[Aoda-Nal-β ³ Leu-Ala]	17 ± 2	8 ± 1	32 ± 1	ND	> 10000
9 c[Asu-Nal-β ³ Trp-Phe]	1040 ± 10	460 ± 20	1670 ± 30	ND	(8000)
10 c[Asu-Nal-β ³ Leu-Phe]	253 ± 4	68 ± 3	690 ± 20	530 ± 10	5800 ± 40
11 c[Asu-Nal-β ³ Trp-Aib]	1010 ± 20	(751)	(2990)	(2670)	(3700)
14 c[Asu-Nal-β ³ Leu-Aib]	500 ± 20	136 ± 1	970 ± 10	(870)	(7000)
15 c[Aoda-Trp-β ³ Leu-Lys(Ac)]	ND	42 ± 5	54 ± 5	150 ± 10	> 10000
16 c[Aoda-Trp-β ³ Leu-Aoda]	ND	150 ± 20	260 ± 10	1400 ± 40	> 10000
17 c[Asu-Nal-β ³ Leu-Arg]	ND	(178)	262 ± 3	(607)	1400 ± 20
18 c[Asu-Nal-β ³ Ser-Arg]	ND	ND	1090 ± 10	ND	2320 ± 20
19 c[Asu-Nal-β ³ Tyr-Arg]	ND	ND	694 ± 4	(1400)	1080 ± 20
20 c[Asu-Nal-β ³ Tyr-Lys(Ac)]	ND	288 ± 4	1040 ± 20	(1380)	4400 ± 30
21 c[Asu-Nal-β ³ Tyr-Phe(F ₅)]	ND	(~1000)	3630 ± 20	(6700)	> 10000
22 c[Asu-Asp-β ³ Tyr-Arg]	ND	> 10000	> 10000	ND	> 10000
23 c[Asu(NHOH)-Asp-β ³ Tyr-Arg]	ND	120 ± 20	164 ± 4	240 ± 10	39 ± 3
24 c[Aoda-Trp-β ³ Leu-Phe] ^c	ND	ND	ND	ND	ND
25 c[Asu(NHOH)-Trp-β ³ Leu-Phe]	ND	ND	31 ± 5	ND	70 ± 6
26 c[Asu-Nal-β ³ Leu-Lys]	ND	ND	242 ± 5	ND	1120 ± 10
27 c[Asu-Nal-β ³ Leu-Lys(Ac)]	ND	56 ± 4	190 ± 10	1000 ± 20	1670 ± 20
28 c[Cys(Pa)-Trp-β ³ Leu-Lys(Ac)]	ND	ND	> 10000	7040 ± 50	> 10000
1a apicidin	22 ± 6	22 ± 4	29 ± 4	760 ± 20	> 10000
TSA	3 ± 1.3	3.3 ± 1.5	11 ± 1.4	25 ± 3	6 ± 1.9

^a IC₅₀ values are means of at least two experiments performed in duplicate. Values in parentheses are from a single assay performed at least in duplicate. ND = not determined. Pa = 3-propanoic acid (see Figure 1 for structure). ^b In complex with NCoR2. ^c This compound was too hydrophobic for assaying.

various nonribosomal cyclic tetrapeptide inhibitors and their analogues (mostly hydrophobic residues), a number of hydrophilic residues (i.e., β³Ser, Thr, Arg, and Lys) were included due to the presence of these side chains in the histone tails (SI Figure S1). Aspartic acid was also included due to its presence vicinal to an N^ε-acetylated lysine in α-tubulin, which is known to be a substrate for HDAC6.

A 525-member second-generation library (Figure 4) was next synthesized on macrobeads as described for the initial library. The compounds were initially screened for HDAC inhibition activity in HeLa cell extract, and then both libraries were counter-screened against HDAC6. As before, the hits were confirmed by retesting the stock solutions in duplicate as well as performing LC-MS/MS sequencing and MALDI-TOF MS, which furnished another nine hit structures (for full hit series, see SI Figures S6 and S7). All the hits contained either Trp or naphthylalanine at the aa2 position. In addition to the results already discussed for the first generation library above, Tyr at the aa3 position was observed in a number of hits, while Phe(F₅) or Arg appeared at the aa4 position. Unfortunately, no hits against HDAC6 were observed that were not also inhibitors of HeLa HDAC activity. Three peptides that were hits against both HeLa extract and HDAC6, all of which had an Arg residue at the aa4 position, were resynthesized (compounds **17–19**) along with two analogues having either a Lys(Ac) or a Phe(F₅) residue at the aa4 position, respectively (compounds **20**, **21**) (Figure 5 and Table 2). The obtained IC₅₀ values revealed that the unnatural Phe(F₅) residue, which was present in a number of hits from the HeLa HDAC activity screening, resulted in low potency of compound **21** over the whole selection of enzyme isoforms tested, so other hit structures containing this residue were not pursued further.

Structure–Activity Relationships and HDAC Isoform Selectivity. The compounds differing only in the identity of the residue at position aa3 (**17–19**) revealed interesting SAR information. Notably, the compound having the β³Tyr–Arg

**Figure 4.** Amino acids included in the second-generation tetrapeptide library (525 members).

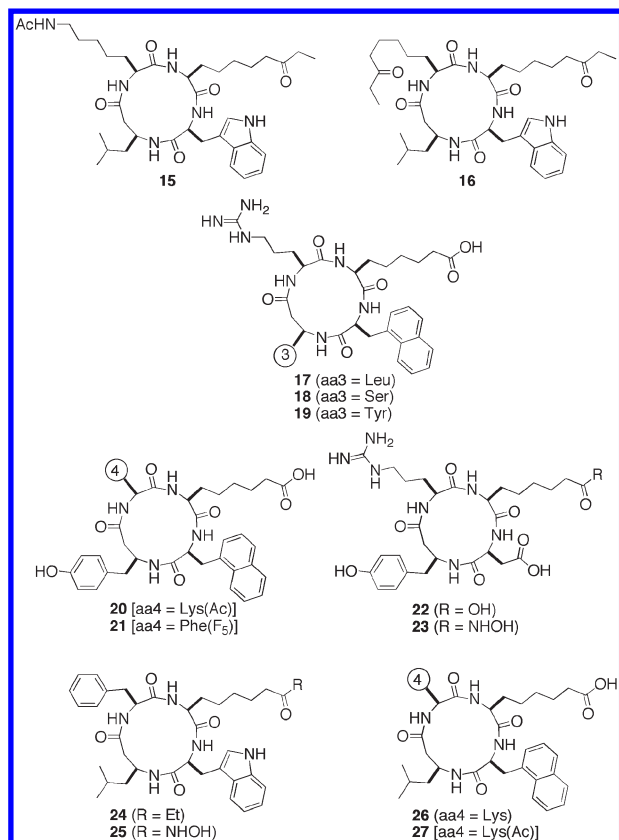


Figure 5. Chemical structures of peptide ligands.

motif at positions aa3–aa4 (**19**) was the most potent carboxylic acid-containing inhibitor of HDAC6 identified so far and had also the best selectivity index (HDAC3/HDAC6 = 0.65) in the series, albeit still in favor of the class I HDACs. Because HDAC6 is known to deacetylate α -tubulin, we decided to combine the β^3 Tyr–Arg motif with an Asp residue at the aa2 position to give compounds **22** and **23**. Interestingly, a successful reversal of the isoform selectivity pattern was achieved with compound **23**, as the selectivity indices for HDAC1/HDAC6, HDAC3/HDAC6, and HDAC8/HDAC6 were approximately 3, 4, and 6, respectively, with potent inhibition of HDAC6 (IC_{50} = 39 nM). Compound **23** is, to the best of our knowledge, the first cyclic tetrapeptide analogue exhibiting isoform selectivity toward a class II HDAC. Moreover, its selectivity index is comparable to that observed for tubacin (HDAC1/HDAC6 selectivity index of 7),^{75–77} and its potency is in the nanomolar range as recently reported for a series of thiolate containing inhibitors^{78,79} inspired by an HDAC6 selective substrate.^{80,81} More potent (picomolar) HDAC6 selective inhibitors containing a phenylisoxazole surface recognition group have also been reported recently.⁸² The ethylketone analogue **24** containing the aa4–Phe residue as observed in compound **10** was prepared in the hopes that higher potency against HDAC1 could be obtained while still retaining the selectivity profile discussed for **10**, but peptide **24** was unfortunately too hydrophobic and hence insoluble under the assay conditions. As expected based on previously observed trends for hydroxamic acid compound **3c**, the hydroxamic acid containing homologue **25** was a potent inhibitor of both classes of HDACs.

To derive more detailed SAR related to compounds **17**, **19**, and **20**, we also prepared peptides **26** and **27** containing the

Lys–aa4 and the Lys(Ac)–aa4 residues, respectively. The potencies of these compounds confirm that an aromatic residue at position aa3 results in decreased potency against the class I HDACs, as previously observed for **9–14**. Furthermore, the results show that substitution of the Lys(Ac)–aa4 residue (**27**) for an Arg–aa4 (**17**) or a Lys–aa4 residue (**26**) had little effect on the inhibitory activities measured against the entire selection of HDACs. It was recently reported that an Arg residue vicinal to the Lys(Ac) promoted binding of synthetic histone substrates to HDAC8,⁸³ which also corresponds well with the observation that most of the lysine residues known to participate in acetylation/deacetylation events in the tails of histones H3, H4, and H2A have Arg residues in their vicinity (SI Figure S1). Taking into account that compounds **17**, **26**, and **27** are also 4–5-fold more potent against HDAC3 and 3–4-fold more potent against HDAC6 when compared to their Ala–aa4 analogue (**8b**), our results suggest that the presence of an Arg, Lys, or Lys(Ac) residue vicinal to the Zn^{2+} -coordinating amino acid may also promote binding to other HDAC isoforms (i.e., HDACs 3 and 6 in this study). To check if the Lys(Ac) residue in **27** was deacetylated under the conditions of our assay, we carried out the standard HeLa extract assay with this compound (at concentrations of 10 μ M or 1 μ M), but instead of the trypsin development step, we quenched the reaction with MeOH and analyzed the reaction mixtures by LC-MS. These experiments showed the peak expected for compound **27** but no trace of the corresponding deacetylated analogue (**26**).

Finally, the composition of our most potent inhibitor of HDAC8 (compound **15**) was combined with the cysteine derived Zn^{2+} -coordinating amino acid containing one methylene unit fewer than Asu (as in **4c**) to give peptide **28**. Although the HDAC3/HDAC8 selectivity was reversed, the potency against HDAC8 was not considered satisfactory. Efforts to design cyclic tetrapeptide inhibitors with improved potency as well as selectivity for HDAC8 are now in progress in our laboratory. The SAR information obtained is summarized in Figure 6.

Western Blot Analysis and Cell Growth Inhibition. To assess the effectiveness of our novel inhibitors in cells, we treated Jurkat cells (T-cell leukemia) with a selection of compounds (apicidin **1a**, **10**, **15**, and **23**) for 24 h and Western blotted for histone H3, acetylated histone H3 (K9 + K14), and acetylated α -tubulin as previously described.⁸⁴ The presence of acetylated tubulin is an indicator of HDAC6 inhibition, whereas the presence of acetylated histone H3 indicates inhibition of the class I HDACs. Similarly, as expected based on the IC_{50} values obtained with the recombinant enzyme isoforms, the two ketone containing compounds (apicidin and **15**) exhibited potent histone deacetylase activity and only minor tubulin deacetylase activity. We were also pleased to find that library hit **10**, containing the carboxylic acid Zn^{2+} -coordinating group, affected the acetylated histone levels in the cells compared to the DMSO control, whereas the effect on acetylated α -tubulin levels was considerably less pronounced in relation to the corresponding DMSO control. As expected, considering the in vitro enzyme inhibition data, **10** was less potent than both apicidin and **15** (Figure 7). Finally, the HDAC6 selectivity of compound **23** was confirmed by the presence of relatively high levels of acetylated α -tubulin, with comparably low levels of histone H3 acetylation.

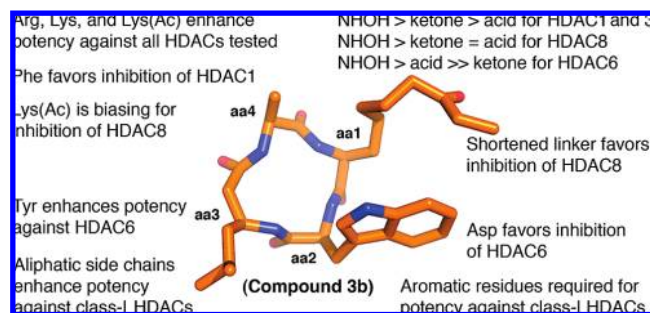


Figure 6. Summary of the obtained SAR information. The shown high-resolution NMR structure of lead compound **3b** in DMSO- d_6 was determined previously by our group.⁶⁷ The hydrogen atoms are omitted for clarity.

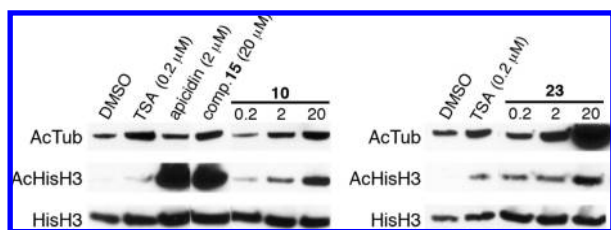


Figure 7. Western blot analysis of lysates from Jurkat cells treated with selected compounds and controls. Concentrations of compounds **10** and **23** are shown in μM . The presence of acetylated tubulin is an indicator of HDAC6 inhibition, whereas the presence of acetylated histone H3 indicates inhibition of the class I HDACs. Histone H3 (bottom) serves as a control for protein loading.

Table 3. GI_{50} Values [μM] for Selected Compounds against Various Cancer Cells^a

compd	HeLa	MCF-7	Jurkat	K-562	KYO-1
vinblastine	0.06	~10	<0.01	0.3	<0.1
1a apicidin	3	7	4	0.9	2.5
3b	3.5 ^b	>20 ^b	ND ^c	2 ^b	10.5 ^b
3c	5.6 ^b	0.6 ^b	1.7	1.6 ^b	0.8 ^b
8b	18	ND	0.3	30	43
10	>20	>20	>20	>20	>20
15	>20	>20	>20	ND	ND
23	9	>20	>20	ND	ND
25	ND	ND	1.3	1.9	1.9

^aHeLa (cervical cancer), MCF-7 (breast cancer), Jurkat (T-cell leukemia), K-562 and KYO-1 (chronic myeloid leukemia). ^bFrom our previous report.⁶⁷ ^cND = not determined.

Growth inhibition of various cancer cell lines by selected compounds was next determined using the XTT assay (Table 3).^{67,85} Except for the highly potent hydroxamic-acid-containing broad spectrum HDAC inhibitors (**3c** and **25**), which were also broadly cytotoxic, the general trend seemed to be that cytotoxicity correlated largely with potent HDAC1 inhibition. Our most potent carboxylic acid HDAC inhibitor (**10**) did not potently inhibit the growth in any of our series of cancer cells, which is in accord with the relatively weak inhibition of HDAC activity in Jurkat cells compared to compound **15** and apicidin indicated by the Western blot. Interestingly, compound **15**, which is an analogue of **3b** with slightly lower potency against HDAC1 (~2-fold) and significantly higher potency against HDAC8 (~15-fold), was less cytotoxic than **3b** toward HeLa cells, indicating that HDAC8 may not be important for cell survival in this cell line. Moreover, compound **23**, which is a >250-fold more potent inhibitor of HDAC6 than **3b** and only ~5-fold less

potent against HDAC1, was less cytotoxic toward HeLa cells than **3b**, indicating that HDAC6 is less important than HDAC1 for cell survival. Clearly, these findings require further support, and differences in cell permeability may also play a major role in the different cytoselectivity profiles observed. In Jurkat cells, for example, compound **8b** proved slightly more potent than the hydroxamic acid inhibitor **3c**, even though **3c** is a more potent inhibitor of all the HDACs tested in vitro. This observation may be explained by an expected more favorable logP value for compound **8b**. The trend observed for these compounds against HeLa, K-562, and KYO-1 cells seem to better reflect the HDAC inhibitory activities, confirming that several factors play important roles in the growth inhibition process. Taken together with the Western blots, these results show that our compounds may find use as specific small-molecule probes to regulate histone and/or tubulin acetylation at subcytotoxic concentrations in cells. Finally, we were pleased to find that by reintroducing the strong Zn^{2+} -coordinating hydroxamic acid moiety in one of the hit compounds to give **25**, we were able to obtain potent growth inhibition in a number of cell lines. This provides further evidence that the effects of the cyclic peptide core and the Zn^{2+} -coordinating moiety on potency may be considered somewhat additive in this class of compounds.

Conclusions

A synthetic tetrapeptide scaffold having an $\alpha\rightarrow\beta$ -amino acid substitution in the backbone has been employed for the identification of moderately selective inhibitors for the HDAC isoforms 1 and 6. Using an all (*S*)-configured $\alpha_3\beta$ ring type as the lead compound, a semihigh-throughput screening scheme was developed for assaying ligands from focused *one-bead-one-compound* libraries. The present study shows that this screening platform in combination with sequence information from natural as well as synthetic HDAC substrates and inhibitors is useful for the discovery of new HDAC inhibitors. The obtained SAR information revealed a range of potent compounds displaying novel side chain patterns and containing unnatural amino acid residues. Depending on the HDAC isoform in question, different amino acid positions on the scaffold proved more or less important for potency, which will aid the future design of selective ligands, help identify optimal sites for labeling, and enable the design of efficient probes for activity-based proteomics or affinity matrix pull-down studies.^{41,86,87}

Our data also indicate that the cyclic tetrapeptide motif not only provides a highly modular scaffold but also that this class of compounds can be further modulated by changing the Zn^{2+} -coordinating moiety in order to fine-tune potency, HDAC isoform selectivity, or cytoselectivity. Importantly, compounds exhibiting potent HDAC inhibitory activity and isoform selectivity were identified and shown to work in cell culture. It is remarkable that from this relatively small selection of compounds, it was possible to design ligands with completely reversed selectivity profiles as compared to the known natural product tetrapeptide inhibitors. We therefore envision that this discovery platform may find additional use for the design of class- and isoform-selective HDAC inhibitors targeting other enzyme isoforms. It will be interesting to explore trends in cytoselectivity between different cell lines in greater detail with these ligands because such studies will help delineate the significance of individual HDACs in

various cancers. This knowledge may aid the design of targeted drug candidates with lower toxicity and fewer side effects.

Experimental Section

Enzymes and Chemicals. HDAC1, HDAC3–NCoR2, HDAC6, and HDAC8 were purchased from BPS Biosciences (San Diego, CA). Trypsin (TPCK treated, from bovine pancreas; 12500 units/mg) was from Sigma-Aldrich (Milwaukee, WI). 2-Cl-Trityl chloride resin macrobeads were from Peptides International (Louisville, KY). Weinreb amide resin was from Novabiochem (San Diego, CA), and 2-chlorotrityl *N*-Fmoc-hydroxylamine resin was from Sigma-Aldrich (Milwaukee, WI). β -Amino acids were purchased from Peptech Corporation (Burlington, MA). All α -amino acids, chemicals, and solvents were used as received from suppliers. HDAC assay buffer was prepared as described in the Biomol International protocol AK-503 (Tris/Cl (50 mM), NaCl (137 mM), KCl (2.7 mM), MgCl₂ (1 mM), pH 8.0). Histone H3 antibody was from Abcam (Cambridge, MA), acetylated K9 + K14 histone antibody was from Upstate (Temecula, CA), and acetylated α -tubulin antibody was from Sigma (St. Louis, MO).

Library Synthesis. *N*-Fmoc-(*S*)-2-Asu(*t*-Bu)-OAllyl (3 equiv with respect to the resin) was stirred in TFA–CH₂Cl₂ for 1 h,⁷³ the solvents were evaporated in vacuo, and the residue was coevaporated several times with CH₂Cl₂–hexane and dried for 2 h under high vacuum. The TFA-free residue was taken up in CH₂Cl₂ (2 mL/100 mg) and *i*-Pr₂EtN (20 equiv) and was shaken with 2-Cl-trityl chloride macrobeads in a fritted syringe for 16 h. The resin was washed with DMF, MeOH, and CH₂Cl₂ (3× each), and the loading was determined by UV measurement (290 nm) of the chromophore in an Fmoc deprotected sample (Novabiochem procedure). The bulk of the resin was then Fmoc deprotected with DMF–piperidine (3:1, 2 × 20 min), washed with DMF, MeOH, and CH₂Cl₂ (3× each), and dried in vacuo. Three cycles of combinatorial split–pool Fmoc peptide synthesis were then performed in 3 mL fritted syringes, applying the Fmoc protected amino acids (5 equiv), DIC (5 equiv), HOBt (5 equiv), and bromophenol blue (2 equiv) as internal indicator in each coupling step.⁸⁸ Standard Fmoc deprotection and washing protocols were applied. After coupling of the fourth amino acid, the resins were washed with DMF, MeOH, CH₂Cl₂, and CHCl₃–*N*-methylmorpholine degassed with argon (3× each). The allyl group was then cleaved with Pd(Ph₃P)₄ (0.2 equiv) in degassed CHCl₃–*N*-methylmorpholine (4 mL) by shaking for 16 h in the dark, after which time the resin was washed with DMF, 1% sodium dimethylthiocarbamate in DMF, and then neat DMF again (2× each), followed by Fmoc deprotection and standard washing. Finally, the resin-bound peptides were cyclized (2 × 12 h) with HATU (5 equiv) and *i*-PrEt₂N (20 equiv) in DMF (3 mL), washed extensively, and dried under high vacuum. The beads were then divided into individual wells in round-bottomed 96-well polypropylene microtiter plates (Fisherbrand), leaving a column free for the standards and controls during screening. To each well was added ~200 μ L of a cleavage cocktail (TFA–CH₂Cl₂–*i*-Pr₂SiH–H₂O (48:48:2:2)) and the plates were left for 16 h. Residual solvents were removed by placing the plates under vacuum in a desiccator for 24 h, before DMSO was added to give stock solutions (1 mM theoretical concentration based on the initial loading and beads/mg) of each peptide for screening and sequencing.

Peptide Synthesis. Compounds were prepared on solid phase with cyclization on the resin (for hydroxamic acids) or in solution (for ethylketones) as previously described.⁶⁷ Linear precursors for carboxylic-acid-containing pseudopeptides were prepared by standard Fmoc SPPS and cleaved using 2,2,2-trifluoroethanol–HOAc–CH₂Cl₂ (2:2:6) in order to keep the side chain protecting groups in place until after cyclization in solution. All compounds were purified to homogeneity by

Table 4. Data for Resynthesized Peptides

compd	HPLC _{230 nm} , %	ESI-TOF HRMS calcd/found (<i>m/z</i>)
4a	99	608.2883/608.2893 ^a
4b	95	594.2721/594.2721 ^a
4c	96	582.2357/582.2348 ^a
4d	90	568.2200/568.2198 ^a
8a	99	589.2997/589.2996 ^a
8b	99	579.3541/579.3537 ^b
9	90	738.3268/738.3280 ^a
10	99	665.3310/665.3298 ^a
11	95	654.3286/654.3285 ^b
14	95	603.3153/603.3197 ^a
15	99	689.3997/689.3992 ^a
16	99	702.4201/702.4197 ^a
17	99	652.3812/652.3814 ^b
18	96	626.3297/626.3300 ^b
19	99	702.3610/702.3617 ^b
20	99	716.3654/716.3658 ^b
21	95	783.2812/783.2821 ^b
22 ^c	95	620.3039/620.3027 ^b
23 ^c	90	635.3148/635.3147 ^b
24 ^c	95	644.3806/644.3794 ^b
25	95	647.3557/647.3552 ^b
26 ^c	95	624.3756/624.3759 ^b
27 ^c	92	666.3861/666.3867 ^b
28	95	681.3041/681.3039 ^a

^a[M + Na]⁺. ^b[M + H]⁺. ^c¹H NMR spectra are included in the Supporting Information

preparative reversed-phase HPLC (C-18 column), and the obtained fractions were lyophilized to give the compounds as fluffy solids that were characterized by LC-MS and high resolution ESI-TOF MS (Table 4) as well as ¹H NMR for selected compounds. The purities of the compounds were determined by analytical HPLC with UV detection at 230 nm, using a Phenomenex Luna 150 mm × 4.6 mm C18(2) column (5 μ) eluted at a rate of 1.5 mL/min. Injection volumes were 20 μ L of approximately 1 mg/mL solution. The gradient elution system consisted of eluent A (H₂O–MeCN–TFA 99:1:0.1) and eluent B (MeCN–H₂O–TFA 90:10:0.07) rising linearly from 0% to 100% of B during 30 min. All cyclic peptides were \geq 95% pure, with the exceptions of compounds **4d**, **9**, **23**, and **27**, which were \geq 90% pure. The HPLC purity of each compound is given in Table 4. DMSO stock solutions were prepared using UV (ϵ (Trp) = 5690 M⁻¹ × cm⁻¹ (280 nm) and ϵ (Tyr) = 1280 M⁻¹ × cm⁻¹ (280 nm)) to adjust the concentrations. Stock solutions of compounds lacking these aromatic chromophores were prepared by weight.

IC₅₀ Determination. The IC₅₀ values against HeLa extracts were determined using the standard Biomol HDAC fluorimetric assay protocol (AK-503).⁸⁵ For inhibition of recombinant human HDACs, the dose–response experiments with internal controls were performed in black or white low binding Nunc 96-well microtiter plates. The dilution series were prepared in Milli-Q water from 1 mM DMSO stock solutions. The appropriate dilution of the inhibitor (10 μ L of a 5× concentration solution) was added to each well followed by HDAC assay buffer (37.5 μ L) containing Ac-Lys(Ac)-AMC substrate (67 μ M) and bovine serum albumin (0.75 mg/mL). For HDAC8, the Arg-His-Lys(Ac)-Lys(Ac)-AMC substrate (27 μ M) was used. Finally, a solution of the appropriate HDAC (2.5 μ L) was added and the plate was incubated at 37 °C for 30 min in the dark (HDAC1, 0.09 μ g/ μ L; HDAC3, 0.03 μ g/ μ L; HDAC6, 0.011 μ g/ μ L; HDAC8, 0.4 μ g/ μ L). Then trypsin (50 μ L, 0.4 mg/mL) was added and the assay development was allowed to proceed for 15 min at RT before the plate was read using a Tecan GENios plate reader with excitation at 360 nm and detecting emission at 460 nm.

Library Screening and Hit Identification. Dilutions of 10 and 1 μM were prepared from each of the 1 mM DMSO stock solutions, and 10 μL of each were added to white Nunc assay plates. In each plate, standards and controls consisted of duplicate wells of: (1) no enzyme (blank), (2) 1 μM of inhibitor **3a**, (3) 1 μM of apicidin, or (4) no inhibitor (max read-out) were installed in each plate. For screening of HDAC6, we used TSA (0.1 μM) instead of apicidin as one of the internal standards. Each plate was assayed as described above for the purified peptides, and compounds that were considered hits, i.e., satisfied our criteria for inhibition at both concentrations, were rediluted and retested in duplicate to weed out false positives. Hits that also satisfied this round of screening were then sequenced using automated LC-MS/MS as previously described,^{74,89–91} and parent ion masses were confirmed by either negative mode sonic spray ionization (SSI) MS or MALDI-TOF MS.

Western Blot Analysis. Jurkat cells were cultivated in RPMI 1640 medium supplemented with 10% fetal bovine serum and antibiotics. At confluency, cells were seeded in six-well plates and incubated with various concentrations of the inhibitor compounds at 37 °C for 24 h. The cells were then washed, harvested, and lysed. The lysates were run on 4–12% polyacrylamide SDS PAGE gels (Invitrogen), transferred to nitrocellulose membranes, and visualized as described previously.⁸⁴ TSA and the vehicle (DMSO) were used as positive and negative controls, respectively.

Cancer Cell Cytotoxicity Assays. Cells were cultivated in flat 96-well tissue culture plates in 90 μL of medium supplemented with 10% FBS and antibiotics. HeLa cells were seeded at a density of 5000 cells/well, Jurkat and MCF-7 at a density of 10000 cells/well, and K-562 and KYO-1 at a density of 15000 cells/well. Twenty-four hours later, 10 μL of medium containing various concentrations of the desired compounds were added in triplicate, and the cells were incubated at 37 °C for 72 h in a 5% CO atmosphere. Cell survival was determined using the XTT (Sigma-Aldrich, St. Louis, MO) colorimetric assay. Immediately prior to use, a mixture of XTT (1 mg/mL) and PMS (*N*-methyl dibenzopyrazine methyl sulfate, 0.383 mg/mL) in phenol-red-free RPMI was prepared (0.1 mL of PMS per 5 mL of XTT solution). After adding 50 μL of this mixture to each well, plates were incubated at 37 °C for 2 h in the case of HeLa and MCF-7 cells, and 4 h for Jurkat, K-562, and KYO-1 cells. Plates were shaken to evenly distribute the dye in the wells, and the absorbance was measured using a Tecan GENios plate reader spectrometer at a wavelength of 485 nm.

Acknowledgment. We thank the TSRI Mass Spectrometry Facility for high resolution mass spectral analyses, Dr. Ana Montero for cell lines and HeLa cell extracts, Andrei Loutchnikov and Devon Cayer for MCF-7 and Jurkat cell lines, respectively, Prof. Joel M. Gottesfeld, Dr. James C. Chou, and Dr. David Herman for helpful discussions and assistance with western blot analyses, as well as Dr. Luke J. Leman for fruitful discussions and invaluable comments on this manuscript. C.A. O. thanks the Benzon Foundation and the Lundbeck Foundation for postdoctoral fellowships as well as the Danish Independent Research Council for a Young Researcher's Award (274-06-0317). This work was supported in part by a grant from the National Institute of General Medical Sciences (GM52190) and the Skaggs Institute for Chemical Biology.

Supporting Information Available: Figures S1–S7 and ¹H NMR spectra for selected compounds. This material is available free of charge via the Internet at <http://pubs.acs.org>.

References

- (1) Kouzarides, T. Chromatin modifications and their function. *Cell* **2007**, *128*, 693–705.

- (2) Allis, C. D.; Berger, S. L.; Cote, J.; Dent, S.; Jenuwien, T.; Kouzarides, T.; Pillus, L.; Reinberg, D.; Shi, Y.; Shiekhhattar, R.; Shilatifard, A.; Workman, J.; Zhang, Y. New nomenclature for chromatin-modifying enzymes. *Cell* **2007**, *131*, 633–636.
- (3) Biel, M.; Wascholowski, V.; Giannis, A. Epigenetics—an epicenter of gene regulation: histones and histone-modifying enzymes. *Angew. Chem., Int. Ed.* **2005**, *44*, 3186–3216.
- (4) Verdin, E.; Dequiedt, F.; Kasler, H. G. Class II histone deacetylases: versatile regulators. *Trends Genet.* **2003**, *19*, 286–293.
- (5) Yuan, Z. L.; Guan, Y. J.; Chatterjee, D.; Chin, Y. E. Stat3 dimerization regulated by reversible acetylation of a single lysine residue. *Science* **2005**, *307*, 269–273.
- (6) Hubbert, C.; Guardiola, A.; Shao, R.; Kawaguchi, Y.; Ito, A.; Nixon, A.; Yoshida, M.; Wang, X. F.; Yao, T. P. HDAC6 is a microtubule-associated deacetylase. *Nature* **2002**, *417*, 455–458.
- (7) Parmigiani, R. B.; Xu, W. S.; Venta-Perez, G.; Erdjument-Bromage, H.; Yaneva, M.; Tempst, P.; Marks, P. A. HDAC6 is a specific deacetylase of peroxiredoxins and is involved in redox regulation. *Proc. Natl. Acad. Sci. U.S.A.* **2008**, *105*, 9633–9638.
- (8) Pandey, U. B.; Nie, Z.; Batlevi, Y.; McCray, B. A.; Ritson, G. P.; Nedelsky, N. B.; Schwartz, S. L.; DiProspero, N. A.; Knight, M. A.; Schuldiner, O.; Padmanabhan, R.; Hild, M.; Berry, D. L.; Garza, D.; Hubbert, C. C.; Yao, T. P.; Baehrecke, E. H.; Taylor, J. P. HDAC6 rescues neurodegeneration and provides an essential link between autophagy and the UPS. *Nature* **2007**, *447*, 859–863.
- (9) Paris, M.; Porcelloni, M.; Binascchi, M.; Fattori, D. Histone deacetylase inhibitors: from bench to clinic. *J. Med. Chem.* **2008**, *51*, 1505–1529.
- (10) Bieliauskas, A. V.; Pflum, M. K. Isoform-selective histone deacetylase inhibitors. *Chem. Soc. Rev.* **2008**, *37*, 1402–1413.
- (11) Cole, P. A. Chemical probes for histone-modifying enzymes. *Nat. Chem. Biol.* **2008**, *4*, 590–597.
- (12) Bolden, J. E.; Peart, M. J.; Johnstone, R. W. Anticancer activities of histone deacetylase inhibitors. *Nat. Rev. Drug Discovery* **2006**, *5*, 769–784.
- (13) Minucci, S.; Pelicci, P. G. Histone deacetylase inhibitors and the promise of epigenetic (and more) treatments for cancer. *Nat. Rev. Cancer* **2006**, *6*, 38–51.
- (14) Marks, P.; Rifkin, R. A.; Richon, V. M.; Breslow, R.; Miller, T.; Kelly, W. K. Histone deacetylases and cancer: causes and therapies. *Nat. Rev. Cancer* **2001**, *1*, 194–202.
- (15) Marks, P. A.; Richon, V. M.; Breslow, R.; Rifkin, R. A. Histone deacetylase inhibitors as new cancer drugs. *Curr. Opin. Oncol.* **2001**, *13*, 477–483.
- (16) Marks, P. A.; Breslow, R. Dimethyl sulfoxide to vorinostat: development of this histone deacetylase inhibitor as an anticancer drug. *Nat. Biotechnol.* **2007**, *25*, 84–90.
- (17) Kazantsev, A. G.; Thompson, L. M. Therapeutic application of histone deacetylase inhibitors for central nervous system disorders. *Nat. Rev. Drug. Discovery* **2008**, *7*, 854–868.
- (18) Fischer, A.; Sananbenesi, F.; Wang, X.; Dobbin, M.; Tsai, L. H. Recovery of learning and memory is associated with chromatin remodelling. *Nature* **2007**, *447*, 178–182.
- (19) Herman, D.; Jenness, K.; Burnett, R.; Soragni, E.; Perlman, S. L.; Gottesfeld, J. M. Histone deacetylase inhibitors reverse gene silencing in Friedreich's ataxia. *Nat. Chem. Biol.* **2006**, *2*, 551–558.
- (20) Tsankova, N. M.; Berton, O.; Renthal, W.; Kumar, A.; Neve, R. L.; Nestler, E. J. Sustained hippocampal chromatin regulation in a mouse model of depression and antidepressant action. *Nat. Neurosci.* **2006**, *9*, 519–525.
- (21) Finnin, M. S.; Donigian, J. R.; Cohen, A.; Richon, V. M.; Rifkin, R. A.; Marks, P. A.; Breslow, R.; Pavletich, N. P. Structures of a histone deacetylase homologue bound to the TSA and SAHA inhibitors. *Nature* **1999**, *401*, 188–193.
- (22) Somoza, J. R.; Skene, R. J.; Katz, B. A.; Mol, C.; Ho, J. D.; Jennings, A. J.; Luong, C.; Arvai, A.; Buggy, J. J.; Chi, E.; Tang, J.; Sang, B. C.; Verner, E.; Wynands, R.; Leahy, E. M.; Dougan, D. R.; Snell, G.; Navre, M.; Knuth, M. W.; Swanson, R. V.; McRee, D. E.; Tari, L. W. Structural snapshots of human HDAC8 provide insights into the class I histone deacetylases. *Structure* **2004**, *12*, 1325–1334.
- (23) Vannini, A.; Volpari, C.; Filocamo, G.; Casavola, E. C.; Brunetti, M.; Renzoni, D.; Chakravarty, P.; Paolini, C.; De Francesco, R.; Gallinari, P.; Steinkuhler, C.; Di Marco, S. Crystal structure of a eukaryotic zinc-dependent histone deacetylase, human HDAC8, complexed with a hydroxamic acid inhibitor. *Proc. Natl. Acad. Sci. U.S.A.* **2004**, *101*, 15064–15069.
- (24) Schuetz, A.; Min, J.; Allali-Hassani, A.; Schapira, M.; Shuen, M.; Loppnau, P.; Mazitschek, R.; Kwiatkowski, N. P.; Lewis, T. A.; Maglathin, R. L.; McLean, T. H.; Bochkarev, A.; Plotnikov, A. N.; Vedadi, M.; Arrowsmith, C. H. Human HDAC7 harbors a class IIA

- histone deacetylase-specific zinc binding motif and cryptic deacetylase activity. *J. Biol. Chem.* **2008**, *283*, 11355–11363.
- (25) Bottomley, M. J.; Lo Surdo, P.; Di Giovine, P.; Cirillo, A.; Scarpelli, R.; Ferrigno, F.; Jones, P.; Neddermann, P.; De Francesco, R.; Steinkuhler, C.; Gallinari, P.; Carfi, A. Structural and functional analysis of the human HDAC4 catalytic domain reveals a regulatory structural zinc-binding domain. *J. Biol. Chem.* **2008**, *283*, 26694–26704.
- (26) Fischle, W.; Dequiedt, F.; Hendzel, M. J.; Guenther, M. G.; Lazar, M. A.; Voelter, W.; Verdin, E. Enzymatic activity associated with class II HDACs is dependent on a multiprotein complex containing HDAC3 and SMRT/N-CoR. *Mol. Cell* **2002**, *9*, 45–57.
- (27) Fischle, W.; Dequiedt, F.; Fillion, M.; Hendzel, M. J.; Voelter, W.; Verdin, E. Human HDAC7 histone deacetylase activity is associated with HDAC3 in vivo. *J. Biol. Chem.* **2001**, *276*, 35826–35835.
- (28) Lahm, A.; Paolini, C.; Pallaoro, M.; Nardi, M. C.; Jones, P.; Neddermann, P.; Sambucini, S.; Bottomley, M. J.; Lo Surdo, P.; Carfi, A.; Koch, U.; De Francesco, R.; Steinkuhler, C.; Gallinari, P. Unraveling the hidden catalytic activity of vertebrate class IIa histone deacetylases. *Proc. Natl. Acad. Sci. U.S.A.* **2007**, *104*, 17335–17340.
- (29) Vega, R. B.; Matsuda, K.; Oh, J.; Barbosa, A. C.; Yang, X.; Meadows, E.; McAnally, J.; Pomajzl, C.; Shelton, J. M.; Richardson, J. A.; Karsenty, G.; Olson, E. N. Histone deacetylase 4 controls chondrocyte hypertrophy during skeletogenesis. *Cell* **2004**, *119*, 555–566.
- (30) Chang, S.; Young, B. D.; Li, S.; Qi, X.; Richardson, J. A.; Olson, E. N. Histone deacetylase 7 maintains vascular integrity by repressing matrix metalloproteinase 10. *Cell* **2006**, *126*, 321–334.
- (31) Tao, R.; de Zoeten, E. F.; Ozkaynak, E.; Chen, C.; Wang, L.; Porrett, P. M.; Li, B.; Turka, L. A.; Olson, E. N.; Greene, M. I.; Wells, A. D.; Hancock, W. W. Deacetylase inhibition promotes the generation and function of regulatory T cells. *Nat. Med.* **2007**, *13*, 1299–1307.
- (32) Wang, S.; Li, X.; Parra, M.; Verdin, E.; Bassel-Duby, R.; Olson, E. N. Control of endothelial cell proliferation and migration by VEGF signaling to histone deacetylase 7. *Proc. Natl. Acad. Sci. U.S.A.* **2008**, *105*, 7738–7743.
- (33) Schreiber, S. L.; Kapoor, T.; Wess, G., Eds. *Chemical Biology: From Small Molecules to Systems Biology and Drug Design*; Wiley-VCH: Weinheim, 2007; Vol. 2, 303 pp.
- (34) Taori, K.; Paul, V. J.; Luesch, H. Structure and activity of largazole, a potent antiproliferative agent from the Floridian marine cyanobacterium *Symploca* sp. *J. Am. Chem. Soc.* **2008**, *130*, 1806–1807.
- (35) Ying, Y.; Taori, K.; Kim, H.; Hong, J.; Luesch, H. Total synthesis and molecular target of largazole, a histone deacetylase inhibitor. *J. Am. Chem. Soc.* **2008**, *130*, 8455–8459.
- (36) Seiser, T.; Kamena, F.; Cramer, N. Synthesis and biological activity of largazole and derivatives. *Angew. Chem., Int. Ed.* **2008**, *47*, 6483–6485.
- (37) Bowers, A.; West, N.; Taunton, J.; Schreiber, S. L.; Bradner, J. E.; Williams, R. M. Total synthesis and biological mode of action of largazole: a potent class I histone deacetylase inhibitor. *J. Am. Chem. Soc.* **2008**, *130*, 11219–11222.
- (38) Nasveschuk, C. G.; Ungermannova, D.; Liu, X.; Phillips, A. J. A concise total synthesis of largazole, solution structure, and some preliminary structure–activity relationships. *Org. Lett.* **2008**, *10*, 3595–3598.
- (39) Ghosh, A. K.; Kulkarni, S. Enantioselective total synthesis of (+)-largazole, a potent inhibitor of histone deacetylase. *Org. Lett.* **2008**, *10*, 3907–3909.
- (40) Kijima, M.; Yoshida, M.; Sugita, K.; Horinouchi, S.; Beppu, T. Trapoxin, an antitumor cyclic tetrapeptide, is an irreversible inhibitor of mammalian histone deacetylase. *J. Biol. Chem.* **1993**, *268*, 22429–22435.
- (41) Taunton, J.; Hassig, C. A.; Schreiber, S. L. A mammalian histone deacetylase related to the yeast transcriptional regulator Rpd3p. *Science* **1996**, *272*, 408–411.
- (42) Kawai, M.; Rich, D. H.; Walton, J. D. The structure and conformation of HC-toxin. *Biochem. Biophys. Res. Commun.* **1983**, *111*, 398–403.
- (43) Shute, R. E.; Dunlap, B.; Rich, D. H. Analogues of the cytostatic and antimetabolic agents chlomydocin and HC-toxin: synthesis and biological activity of chloromethyl ketone and diazomethyl ketone functionalized cyclic tetrapeptides. *J. Med. Chem.* **1987**, *30*, 71–78.
- (44) Darkin-Rattray, S. J.; Gurnett, A. M.; Myers, R. W.; Dulski, P. M.; Crumley, T. M.; Allocco, J. J.; Cannova, C.; Meinke, P. T.; Colletti, S. L.; Bednarek, M. A.; Singh, S. B.; Goetz, M. A.; Dombrowski, A. W.; Polishook, J. D.; Schmatz, D. M. Apicidin: a novel antiprotozoal agent that inhibits parasite histone deacetylase. *Proc. Natl. Acad. Sci. U.S.A.* **1996**, *93*, 13143–13147.
- (45) Singh, S. B.; Zink, D. L.; Polishook, J. D.; Dombrowski, A. W.; Darkin-Rattray, S. J.; Schmatz, D. M.; Goetz, M. A. Apicidins: Novel cyclic tetrapeptides as coccidiostats and antimalarial agents from *Fusarium pallidoroseum*. *Tetrahedron Lett.* **1996**, *37*, 8077–8080.
- (46) Kranz, M.; Murray, P. J.; Taylor, S.; Upton, R. J.; Clegg, W.; Elsegood, M. R. Solution, solid phase and computational structures of apicidin and its backbone-reduced analogs. *J. Pept. Sci.* **2006**, *12*, 383–388.
- (47) Nakao, Y.; Yoshida, S.; Matsunaga, S.; Shindoh, N.; Terada, Y.; Nagai, K.; Yamashita, J. K.; Ganesan, A.; van Soest, R. W.; Fusetani, N.; Azumamides, A-E histone deacetylase inhibitory cyclic tetrapeptides from the marine sponge *Mycale izuensis*. *Angew. Chem., Int. Ed.* **2006**, *45*, 7553–7557.
- (48) Izzo, I.; Maulucci, N.; Bifulco, G.; De Riccardis, F. Total synthesis of azumamides A and E. *Angew. Chem., Int. Ed.* **2006**, *45*, 7557–7560.
- (49) Maulucci, N.; Chini, M. G.; Micco, S. D.; Izzo, I.; Cafaro, E.; Russo, A.; Gallinari, P.; Paolini, C.; Nardi, M. C.; Casapullo, A.; Riccio, R.; Bifulco, G.; Riccardis, F. D. Molecular insights into azumamide E histone deacetylases inhibitory activity. *J. Am. Chem. Soc.* **2007**, *129*, 3007–3012.
- (50) Wen, S.; Carey, K. L.; Nakao, Y.; Fusetani, N.; Packham, G.; Ganesan, A. Total synthesis of azumamide A and azumamide E, evaluation as histone deacetylase inhibitors, and design of a more potent analogue. *Org. Lett.* **2007**, *9*, 1105–1108.
- (51) Nakao, Y.; Narazaki, G.; Hoshino, T.; Maeda, S.; Yoshida, M.; Maejima, H.; Yamashita, J. K. Evaluation of antiangiogenic activity of azumamides by the in vitro vascular organization model using mouse induced pluripotent stem (iPS) cells. *Bioorg. Med. Chem. Lett.* **2008**, *18*, 2982–2984.
- (52) Furumai, R.; Komatsu, Y.; Nishino, N.; Khochbin, S.; Yoshida, M.; Horinouchi, S. Potent histone deacetylase inhibitors built from trichostatin A and cyclic tetrapeptide antibiotics including trapoxin. *Proc. Natl. Acad. Sci. U.S.A.* **2001**, *98*, 87–92.
- (53) Meinke, P. T.; Colletti, S. L.; Doss, G.; Myers, R. W.; Gurnett, A. M.; Dulski, P. M.; Darkin-Rattray, S. J.; Allocco, J. J.; Galuska, S.; Schmatz, D. M.; Wyvratt, M. J.; Fisher, M. H. Synthesis of apicidin-derived quinolone derivatives: parasite-selective histone deacetylase inhibitors and antiproliferative agents. *J. Med. Chem.* **2000**, *43*, 4919–4922.
- (54) Colletti, S. L.; Myers, R. W.; Darkin-Rattray, S. J.; Gurnett, A. M.; Dulski, P. M.; Galuska, S.; Allocco, J. J.; Ayer, M. B.; Li, C.; Lim, J.; Crumley, T. M.; Cannova, C.; Schmatz, D. M.; Wyvratt, M. J.; Fisher, M. H.; Meinke, P. T. Broad spectrum antiprotozoal agents that inhibit histone deacetylase: structure–activity relationships of apicidin. *Bioorg. Med. Chem. Lett.* **2001**, *11*, 107–111.
- (55) Colletti, S. L.; Myers, R. W.; Darkin-Rattray, S. J.; Gurnett, A. M.; Dulski, P. M.; Galuska, S.; Allocco, J. J.; Ayer, M. B.; Li, C.; Lim, J.; Crumley, T. M.; Cannova, C.; Schmatz, D. M.; Wyvratt, M. J.; Fisher, M. H.; Meinke, P. T. Broad spectrum antiprotozoal agents that inhibit histone deacetylase: structure–activity relationships of apicidin. *Bioorg. Med. Chem. Lett.* **2001**, *11*, 113–117.
- (56) Taunton, J.; Collins, J. L.; Schreiber, S. L. Synthesis of natural and modified trapoxins, useful reagents for exploring histone deacetylase function. *J. Am. Chem. Soc.* **1996**, *118*, 10412–10422.
- (57) Berst, F.; Ladlow, M.; Holmes, A. B. Solid-phase synthesis of apicidin A and a cyclic tetrapeptide analogue. *Chem. Commun.* **2002**, 508–509.
- (58) Shivashimpi, G. M.; Amagai, S.; Kato, T.; Nishino, N.; Maeda, S.; Nishino, T. G.; Yoshida, M. Molecular design of histone deacetylase inhibitors by aromatic ring shifting in chlomydocin framework. *Bioorg. Med. Chem.* **2007**, *15*, 7830–7839.
- (59) Gomez-Paloma, L.; Bruno, I.; Cini, E.; Khochbin, S.; Rodriguez, M.; Taddei, M.; Terracciano, S.; Sadoul, K. Design and synthesis of cyclopeptide analogues of the potent histone deacetylase inhibitor FR255222. *ChemMedChem* **2007**, *2*, 1511–1519.
- (60) Horne, W. S.; Olsen, C. A.; Beierle, J. M.; Montero, A.; Ghadiri, M. R. Probing the bioactive conformation of an archetypal natural product HDAC inhibitor with conformationally homogeneous triazole-modified cyclic tetrapeptides. *Angew. Chem., Int. Ed.* **2009**, *48*, 4718–4724.
- (61) Ying, Y.; Liu, Y.; Byeon, S. R.; Kim, H.; Luesch, H.; Hong, J. Synthesis and activity of largazole analogues with linker and macrocycle modification. *Org. Lett.* **2008**, *10*, 4021–4024.
- (62) Bowers, A. A.; Greshock, T. J.; West, N.; Estiu, G.; Schreiber, S. L.; Wiest, O.; Williams, R. M.; Bradner, J. E. Synthesis and conformation–activity relationships of the peptide isosteres of FK228 and largazole. *J. Am. Chem. Soc.* **2009**, *131*, 2900–2905.
- (63) Bowers, A. A.; West, N.; Newkirk, T. L.; Troutman-Youngman, A. E.; Schreiber, S. L.; Wiest, O.; Bradner, J. E.; Williams, R. M. Synthesis and histone deacetylase inhibitory activity of largazole

- analogs: alteration of the zinc-binding domain and macrocyclic scaffold. *Org. Lett.* **2009**, *11*, 1301–1304.
- (64) Schumann, F.; Muller, A.; Kokschi, M.; Muller, G.; Sewald, N. Are beta-amino acids gamma-turn mimetics? Exploring a new design principle for bioactive cyclopeptides. *J. Am. Chem. Soc.* **2000**, *122*, 12009–12010.
- (65) Glenn, M. P.; Kelso, M. J.; Tyndall, J. D.; Fairlie, D. P. Conformationally homogeneous cyclic tetrapeptides: useful new three-dimensional scaffolds. *J. Am. Chem. Soc.* **2003**, *125*, 640–641.
- (66) Norgren, A. S.; Buttner, F.; Prabpai, S.; Kongsaree, P.; Arvidsson, P. I. Beta2-amino acids in the design of conformationally homogeneous cyclo-peptide scaffolds. *J. Org. Chem.* **2006**, *71*, 6814–6821.
- (67) Montero, A.; Beierle, J. M.; Olsen, C. A.; Ghadiri, M. R. Design, synthesis, biological evaluation, and structural characterization of potent histone deacetylase inhibitors based on cyclic alpha/beta-tetrapeptide architectures. *J. Am. Chem. Soc.* **2009**, *131*, 3033–3041.
- (68) Lam, K. S.; Salmon, S. E.; Hersh, E. M.; Hruba, V. J.; Kazmierski, W. M.; Knapp, R. J. A new type of synthetic peptide library for identifying ligand-binding activity. *Nature* **1991**, *354*, 82–84.
- (69) Yang, W. M.; Tsai, S. C.; Wen, Y. D.; Fejer, G.; Seto, E. Functional domains of histone deacetylase-3. *J. Biol. Chem.* **2002**, *277*, 9447–9454.
- (70) Glenn, M. P.; Kahnberg, P.; Boyle, G. M.; Hansford, K. A.; Hans, D.; Martyn, A. C.; Parsons, P. G.; Fairlie, D. P. Antiproliferative and phenotype-transforming antitumor agents derived from cysteine. *J. Med. Chem.* **2004**, *47*, 2984–2994.
- (71) Simon, M. D.; Chu, F.; Racki, L. R.; de la Cruz, C. C.; Burlingame, A. L.; Panning, B.; Narlikar, G. J.; Shokat, K. M. The site-specific installation of methyl-lysine analogs into recombinant histones. *Cell* **2007**, *128*, 1003–1012.
- (72) Krennhubec, K.; Marshall, B. L.; Hedglin, M.; Verdin, E.; Ulrich, S. M. Design and evaluation of “Linkerless” hydroxamic acids as selective HDAC8 inhibitors. *Bioorg. Med. Chem. Lett.* **2007**, *17*, 2874–2878.
- (73) Kahnberg, P.; Lucke, A. J.; Glenn, M. P.; Boyle, G. M.; Tyndall, J. D.; Parsons, P. G.; Fairlie, D. P. Design, synthesis, potency, and cytoselectivity of anticancer agents derived by parallel synthesis from alpha-aminosuberic acid. *J. Med. Chem.* **2006**, *49*, 7611–7622.
- (74) Redman, J. E.; Wilcoxon, K. M.; Ghadiri, M. R. Automated mass spectrometric sequence determination of cyclic peptide library members. *J. Comb. Chem.* **2003**, *5*, 33–40.
- (75) Haggarty, S. J.; Koeller, K. M.; Wong, J. C.; Butcher, R. A.; Schreiber, S. L. Multidimensional chemical genetic analysis of diversity-oriented synthesis-derived deacetylase inhibitors using cell-based assays. *Chem. Biol.* **2003**, *10*, 383–396.
- (76) Haggarty, S. J.; Koeller, K. M.; Wong, J. C.; Grozinger, C. M.; Schreiber, S. L. Domain-selective small-molecule inhibitor of histone deacetylase 6 (HDAC6)-mediated tubulin deacetylation. *Proc. Natl. Acad. Sci. U.S.A.* **2003**, *100*, 4389–4394.
- (77) Estiu, G.; Greenberg, E.; Harrison, C. B.; Kwiatkowski, N. P.; Mazitschek, R.; Bradner, J. E.; Wiest, O. Structural origin of selectivity in class II-selective histone deacetylase inhibitors. *J. Med. Chem.* **2008**, *51*, 2898–2906.
- (78) Suzuki, T.; Kouketsu, A.; Itoh, Y.; Hisakawa, S.; Maeda, S.; Yoshida, M.; Nakagawa, H.; Miyata, N. Highly potent and selective histone deacetylase 6 inhibitors designed based on a small-molecular substrate. *J. Med. Chem.* **2006**, *49*, 4809–4812.
- (79) Itoh, Y.; Suzuki, T.; Kouketsu, A.; Suzuki, N.; Maeda, S.; Yoshida, M.; Nakagawa, H.; Miyata, N. Design, synthesis, structure–selectivity relationship, and effect on human cancer cells of a novel series of histone deacetylase 6-selective inhibitors. *J. Med. Chem.* **2007**, *50*, 5425–5438.
- (80) Heltweg, B.; Dequiedt, F.; Marshall, B. L.; Brauch, C.; Yoshida, M.; Nishino, N.; Verdin, E.; Jung, M. Subtype selective substrates for histone deacetylases. *J. Med. Chem.* **2004**, *47*, 5235–5243.
- (81) Because the IC₅₀ values for HDAC8 were obtained using a different substrate that gave a better signal–background ratio for this enzyme, we also measured the inhibition constant for **23** against HDAC8 by applying the same substrate as used for HDACs 1, 3, and 6. This IC₅₀ value was in the same range as observed with the HDAC8 specific substrate Ac-Lys(Ac)-AMC (IC₅₀ = 343 nM), which further confirmed the HDAC8/HDAC6 selectivity for compound **23**.
- (82) Kozikowski, A. P.; Tapadar, S.; Luchini, D. N.; Kim, K. H.; Billadeau, D. D. Use of the nitrile oxide cycloaddition (NOC) reaction for molecular probe generation: a new class of enzyme selective histone deacetylase inhibitors (HDACIs) showing picomolar activity at HDAC6. *J. Med. Chem.* **2008**, *51*, 4370–4373.
- (83) Gurard-Levin, Z. A.; Mrksich, M. The activity of HDAC8 depends on local and distal sequences of its peptide substrates. *Biochemistry* **2008**, *47*, 6242–6250.
- (84) Chou, C. J.; Herman, D.; Gottesfeld, J. M. Pimelic diphenylamide 106 is a slow, tight-binding inhibitor of class I histone deacetylases. *J. Biol. Chem.* **2008**, *283*, 35402–35409.
- (85) Wegener, D.; Hildmann, C.; Riester, D.; Schwienhorst, A. Improved fluorogenic histone deacetylase assay for high-throughput screening applications. *Anal. Biochem.* **2003**, *321*, 202–208.
- (86) Salisbury, C. M.; Cravatt, B. F. Activity-based probes for proteomic profiling of histone deacetylase complexes. *Proc. Natl. Acad. Sci. U.S.A.* **2007**, *104*, 1171–1176.
- (87) Salisbury, C. M.; Cravatt, B. F. Optimization of activity-based probes for proteomic profiling of histone deacetylase complexes. *J. Am. Chem. Soc.* **2008**, *130*, 2184–2194.
- (88) Lam, K. S.; Lebl, M.; Krchnak, V. The “One-bead–one-compound” combinatorial library method. *Chem. Rev.* **1997**, *97*, 411–448.
- (89) Dartois, V.; Sanchez-Quesada, J.; Cabezas, E.; Chi, E.; Dubbelde, C.; Dunn, C.; Granja, J.; Gritzen, C.; Weinberger, D.; Ghadiri, M. R.; Parr, T. R., Jr. Systemic antibacterial activity of novel synthetic cyclic peptides. *Antimicrob. Agents Chemother.* **2005**, *49*, 3302–3310.
- (90) Horne, W. S.; Wiethoff, C. M.; Cui, C.; Wilcoxon, K. M.; Amorin, M.; Ghadiri, M. R.; Nemerow, G. R. Antiviral cyclic D,L-alpha-peptides: targeting a general biochemical pathway in virus infections. *Bioorg. Med. Chem.* **2005**, *13*, 5145–5153.
- (91) Fletcher, J. T.; Finlay, J. A.; Callow, M. E.; Callow, J. A.; Ghadiri, M. R. A combinatorial approach to the discovery of biocidal six-residue cyclic D,L-alpha-peptides against the bacteria methicillin-resistant *Staphylococcus aureus* (MRSA) and *E. coli* and the biofouling algae *Ulva linza* and *Navicula perminuta*. *Chem.—Eur. J.* **2007**, *13*, 4008–4013.